IETR

Chambres réverbérantes électromagnétiques : un outil puissant et moderne pour des applications multiples

Philippe.Besnier
@insa-rennes.fr

cnrs
CentraleSupélec
INSA RENNES
Nantes Université
Université de Rennes

04 juin 2024

Agenda

Introduction to RC

Antenna efficiency and antenna patterns in RC

Average absorbing cross-section

Dosimetry

Backscattering measurements

Focalization

Conclusion

RC: definition

- A reverberation chamber consists of an **oversized** Faraday cage
- It relies on a multiple **natural modes** excitation : the EM field is a **combination of one or several modes** in a given state of the chamber
- An **ensemble of states** are obtained through a stirring process (a change of the boundary conditions). Ensemble statistics may reach ideal properties under some conditions.

A starting example : a 1-D cavity

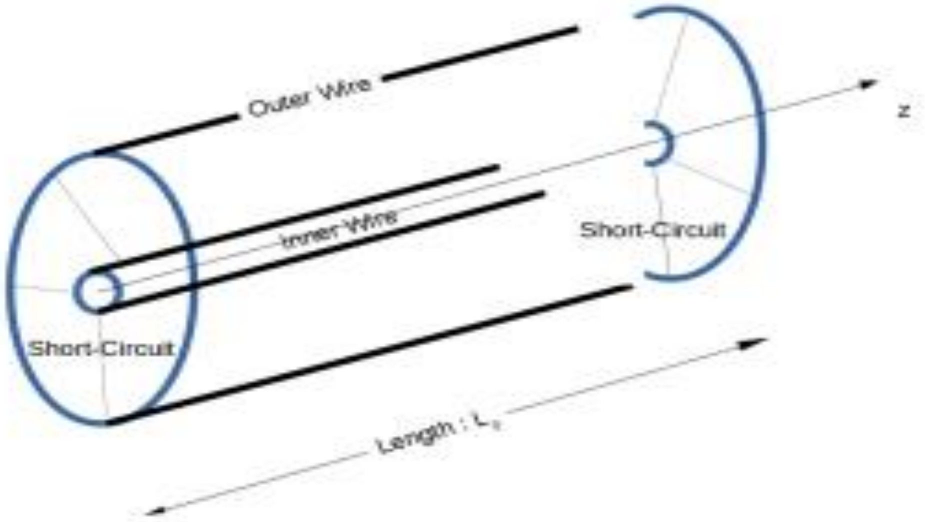

Figure 1 : *A TEM coaxial waveguide*

- A short-circuited coaxial cable (TEM waveguide)

The voltage difference is the solution of the wave equation :

$$V(z) = Z_c \times [A \exp(-\gamma \times z) - B \exp(\gamma \times z)] \tag{1}$$

with $\gamma = jk$ (for a lossless line), k : the wavenumber.
The boundary conditions at $z = 0$ and $z = L_0$ imply :

$$A - B = 0 \tag{2}$$

$$A \exp(-jk \times L_0) - B \exp(-jk \times L_0) = 0 \tag{3}$$

Non trivial solutions appear for a set of eigenvalues k_n :

$$k_n = \frac{n\pi}{L_0} \tag{4}$$

Introduction to RC

Multiple modes
Oversized if L0 high enough

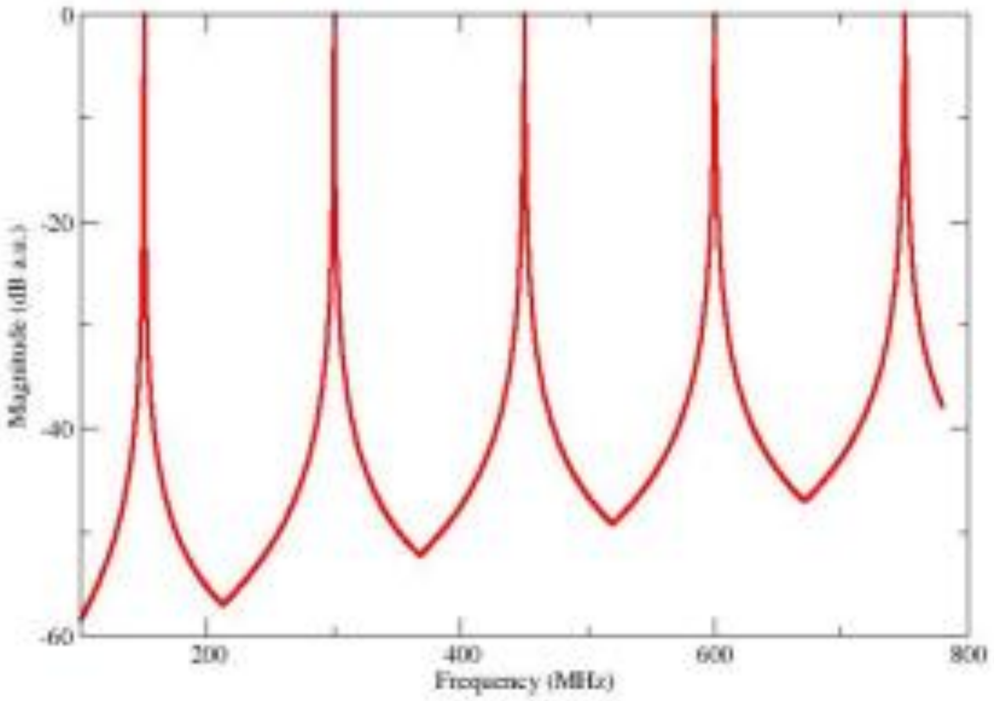

Figure 2 : *First modes of the TEM waveguide with L_0 =1 m. Losses arbitrarily included*

Introduction to RC

Given two short-circuits pistons such that $L_{stir} = L_0 - \delta L$ and δL 20% of L_0 as a maximum :

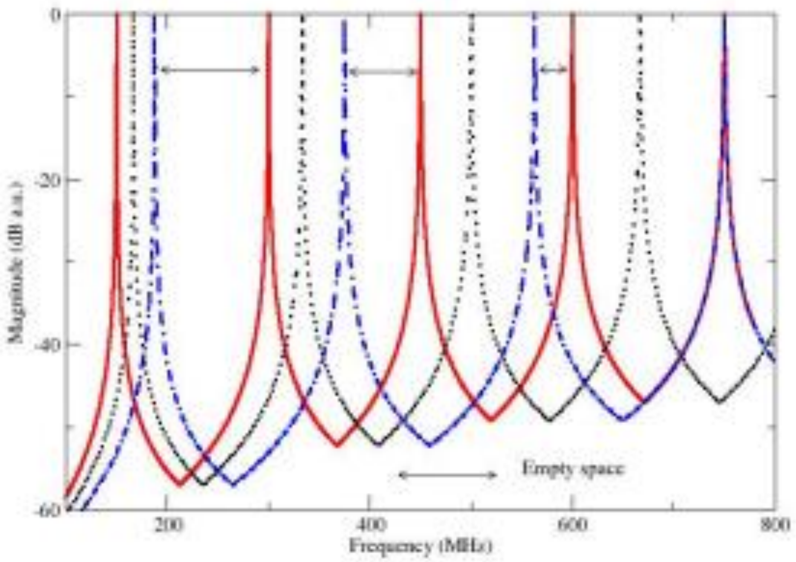

Despite changing b.c. no significant excitation of modes at any frequency at oversized length

Figure 3 : *First modes of the TEM waveguide with L_0 = varying from 1 m to 0.8 m. Losses arbitrarily included*

Introduction to RC

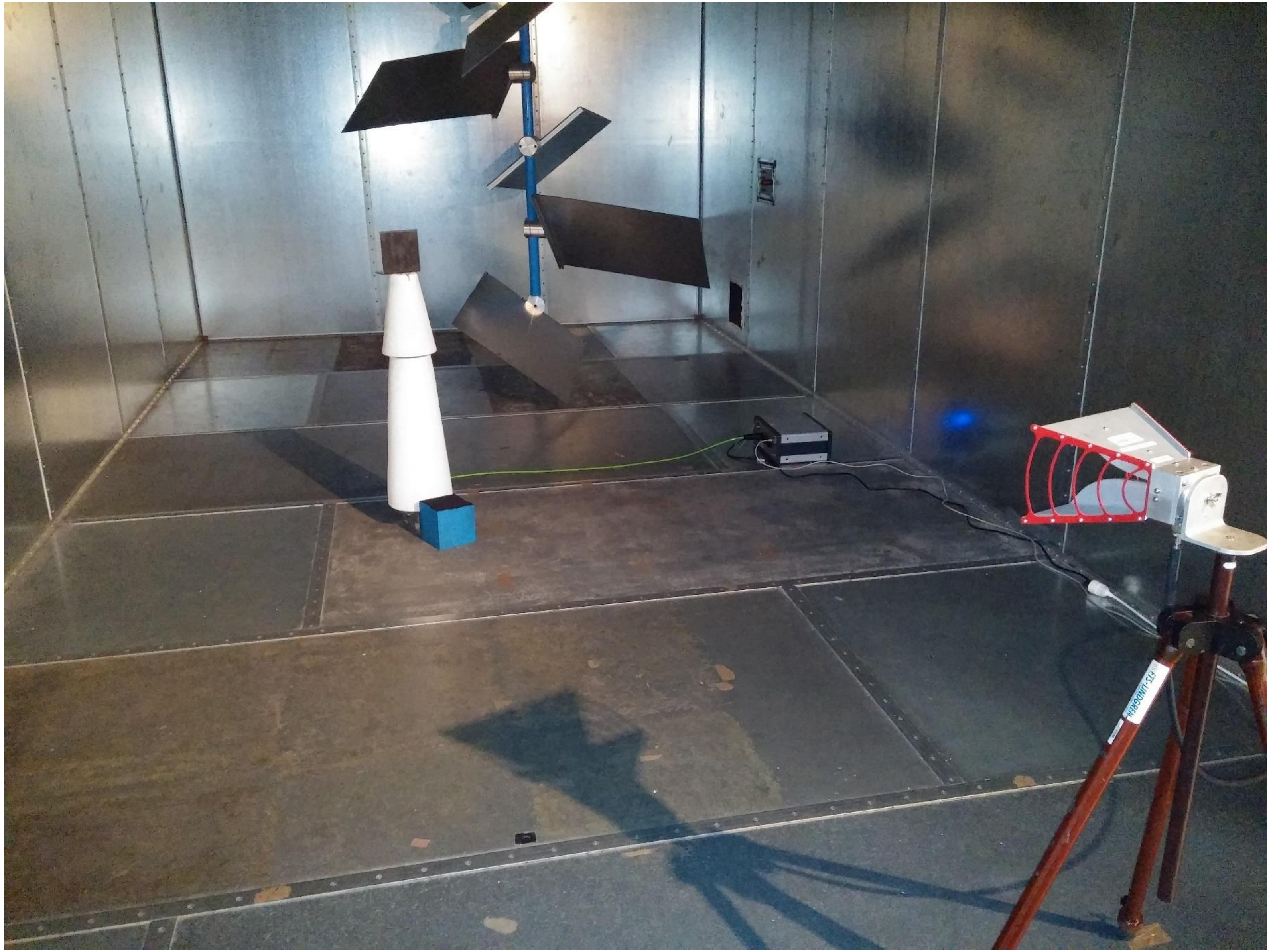

CNRS
CentraleSupélec
INSA Rennes
Nantes Université
Université de Rennes

Introduction to RC

$a = 1.00$ m, $b = 1.05$ m, d=1.10 m (arbitrary losses included) :

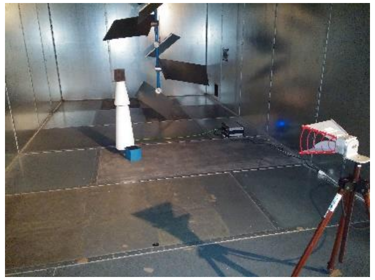

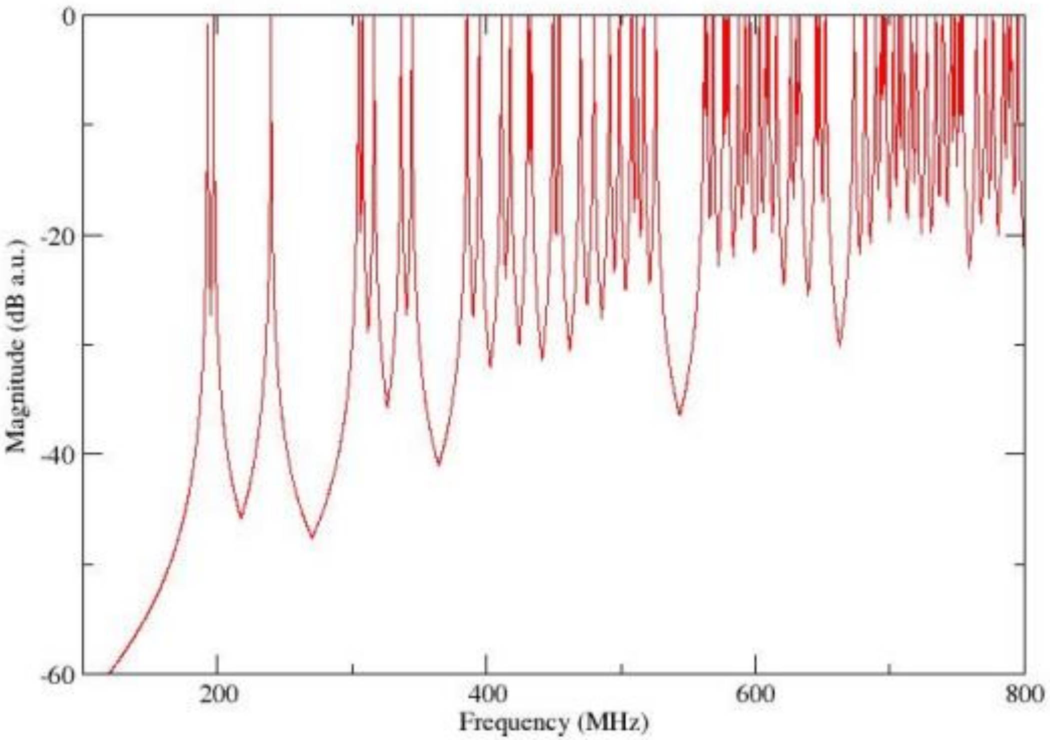

Figure 7 : *A 3D cavity*

Density of modes increases wiith frequency

Introduction to RC

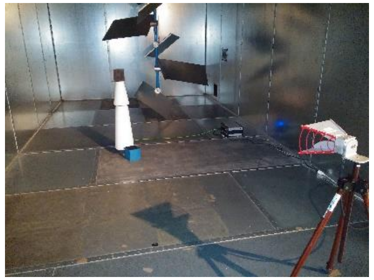

Let imagine a stirring process equivalent to $a = 1.00 + \delta x$, $b = 1.05 + \delta x$, d=$1.10 + \delta x$ with $(\delta x)_{max} = 0.05$ (1% of a).
Suppose a collection of n step variations with step i corresponding to $\delta x = \frac{i}{n}(\delta x)_{max}$

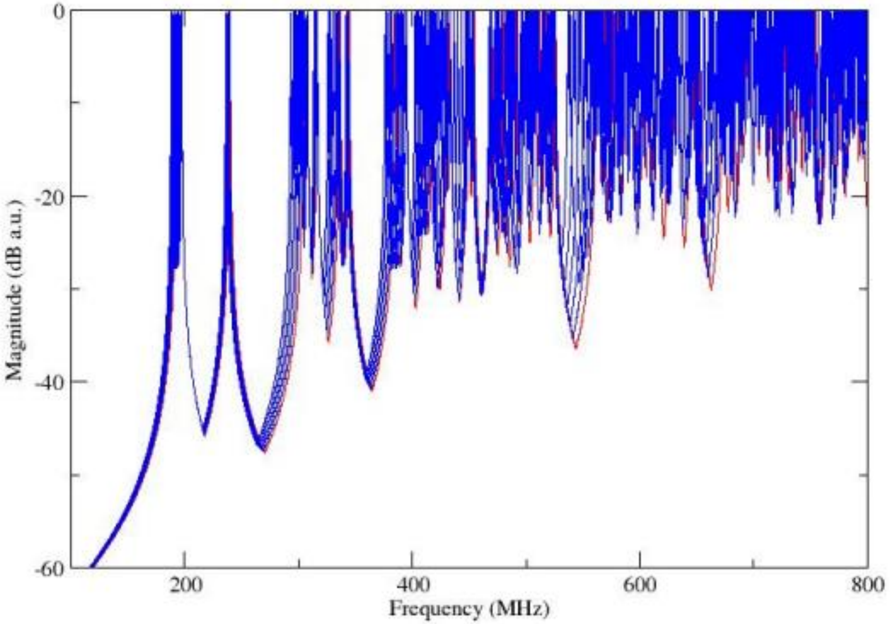

Figure 8 : *Ensemble of modes summing $n = 5$ states of the chamber of a fictitious stirring process*

Introduction to RC

3-D overmoded cavities

- Multiple modes with significant excitation over a number of states

→ Mode density (M) $\approx 8\pi V \frac{f^2}{c}$

→ Composite Q-factor (Q) $= \frac{f}{\Delta f}$

→ $d = M \times \Delta f$ d=<<1

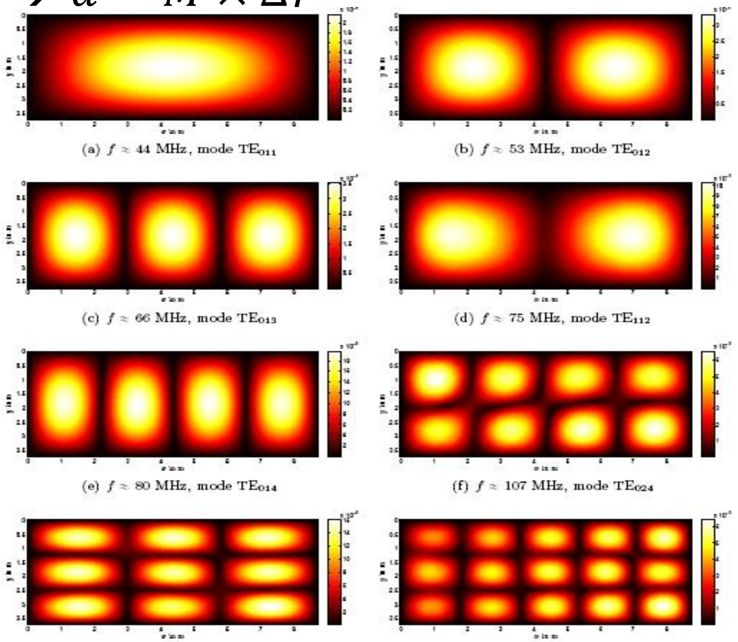

(a) $f \approx 44$ MHz, mode TE_{011} (b) $f \approx 53$ MHz, mode TE_{012}

(c) $f \approx 66$ MHz, mode TE_{013} (d) $f \approx 75$ MHz, mode TE_{112}

(e) $f \approx 80$ MHz, mode TE_{014} (f) $f \approx 107$ MHz, mode TE_{024}

(g) $f \approx 133$ MHz, mode TE_{033} (h) $f \approx 158$ MHz, mode TE_{135}

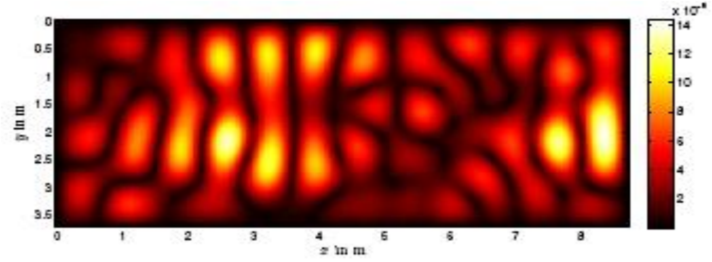

(i) $f \approx 263$ MHz

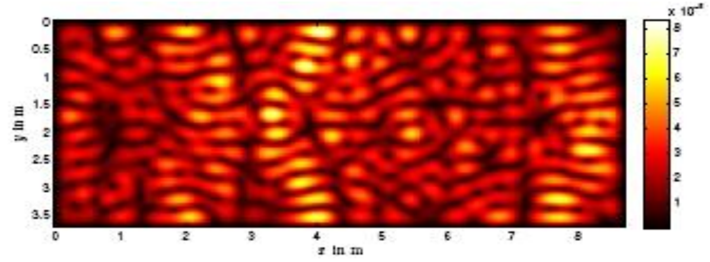

(j) $f \approx 500$ MHz

E. Amador et. al, "Reverberation Chamber Modeling Based on Image Theory: Investigation in the Pulse Regime," in *IEEE Transactions on Electromagnetic Compatibility*, vol. 52, no. 4, pp. 778-789, Nov. 2010

Well overmoded / stirred cavity:

- Plane wave spectrum
- Hill's (asymptotical) model

$$e_{x,y,z}(t) = E_{x,y,z} e^{j\omega t}$$

$$E_{x,y,z} = E^{r}_{x,y,z} + jE^{r}_{x,y,z}$$

$$E^{r}_{x}, E^{r}_{y}, E^{r}_{z}, E^{i}_{x}, E^{i}_{y}, E^{i}_{z} \equiv v$$

$$Var(v) = \sigma_v^{\,2}$$

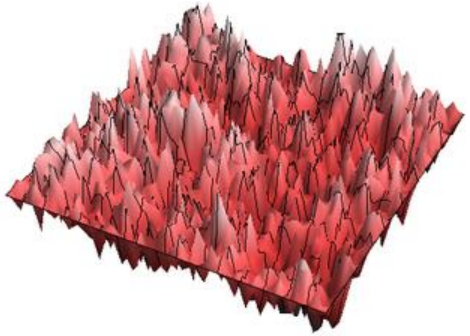

Gaussian « random » field

$$\mathrm{p}_n(v) = \frac{1}{\sqrt{2\pi}\,\sigma_v} e^{-\frac{1}{2}\frac{v^2}{\sigma_v^2}}$$

Q-factor

- Energy is stored in multiple modes
- The higher Q the higher the strored energy and thus the field strength
- The lower Q the higher d (better overlapping situation)
- Depends on losses machanisms

$$Q = \omega_0 \frac{\xi}{P_d}$$

where ξ is the stored energy and P_d the corresponding dissipated power

Q-factor is generally measured as the averaged stored energy over the transmitted/ injected power in the chamber and

$$\frac{1}{Q} = \frac{1}{Q_{walls}} + \frac{1}{Q_{ant}} + \frac{1}{Q_{obj}} \tag{21}$$

Introduction to RC

Antenna effective area $P_{rec} = A_{eff} \times P_{den}$

$$A_{\text{eff}} = \frac{\lambda^2}{4\pi}\eta m[D_\theta(\theta,\phi)\vec{\theta} + D_{phi}(\theta,\phi)\vec{\phi}] \quad (23)$$

The same antenna is now under **a plane wave spectrum illumination.** Its effective area writes :

$$A_{\text{eff}} = \frac{\lambda^2}{4\pi}\eta m \int_0^{2\pi}\int_0^{\pi}[D_\theta(\theta,\phi)p_\theta(\theta,\phi)\vec{\theta} + D_\phi(\theta,\phi)p_\phi(\theta,\phi)\vec{\phi}]\sin\theta d\theta d\phi \quad (24)$$

$p_\theta(\theta,\phi)$ and $p_\phi(\theta,\phi)$ are the probability distribution of the plane wave incidence for each polarization.

$$p_\theta(\theta,\phi) = p_\phi(\theta,\phi) = \frac{1}{4\pi} \quad (25)$$

Receiving antenna $\frac{\lambda^2}{8\pi}\eta m$

(ensemble average)

Transmitting antenna $\frac{\lambda^2}{4\pi}\eta m$

Antenna effective area $P_{rec} = A_{eff} \times P_{den}$

$$A_{\text{eff}} = \frac{\lambda^2}{4\pi}\eta m[D_\theta(\theta,\phi)\vec{\theta} + D_{phi}(\theta,\phi)\vec{\phi}] \tag{23}$$

The same antenna is now under **a plane wave spectrum illumination.** Its effective area writes :

$$A_{\text{eff}} = \frac{\lambda^2}{4\pi}\eta m \int_0^{2\pi}\int_0^{\pi}[D_\theta(\theta,\phi)p_\theta(\theta,\phi)\vec{\theta} + D_\phi(\theta,\phi)p_\phi(\theta,\phi)\vec{\phi}]\sin\theta\, d\theta d\phi \tag{24}$$

$p_\theta(\theta,\phi)$ and $p_\phi(\theta,\phi)$ are the probability distribution of the plane wave incidence for each polarization.

$$p_\theta(\theta,\phi) = p_\phi(\theta,\phi) = \frac{1}{4\pi} \tag{25}$$

Receiving antenna $\frac{\lambda^2}{8\pi}\eta m$ (ensemble average)

Transmitting antenna $\frac{\lambda^2}{4\pi}\eta m$

Introduction to RC

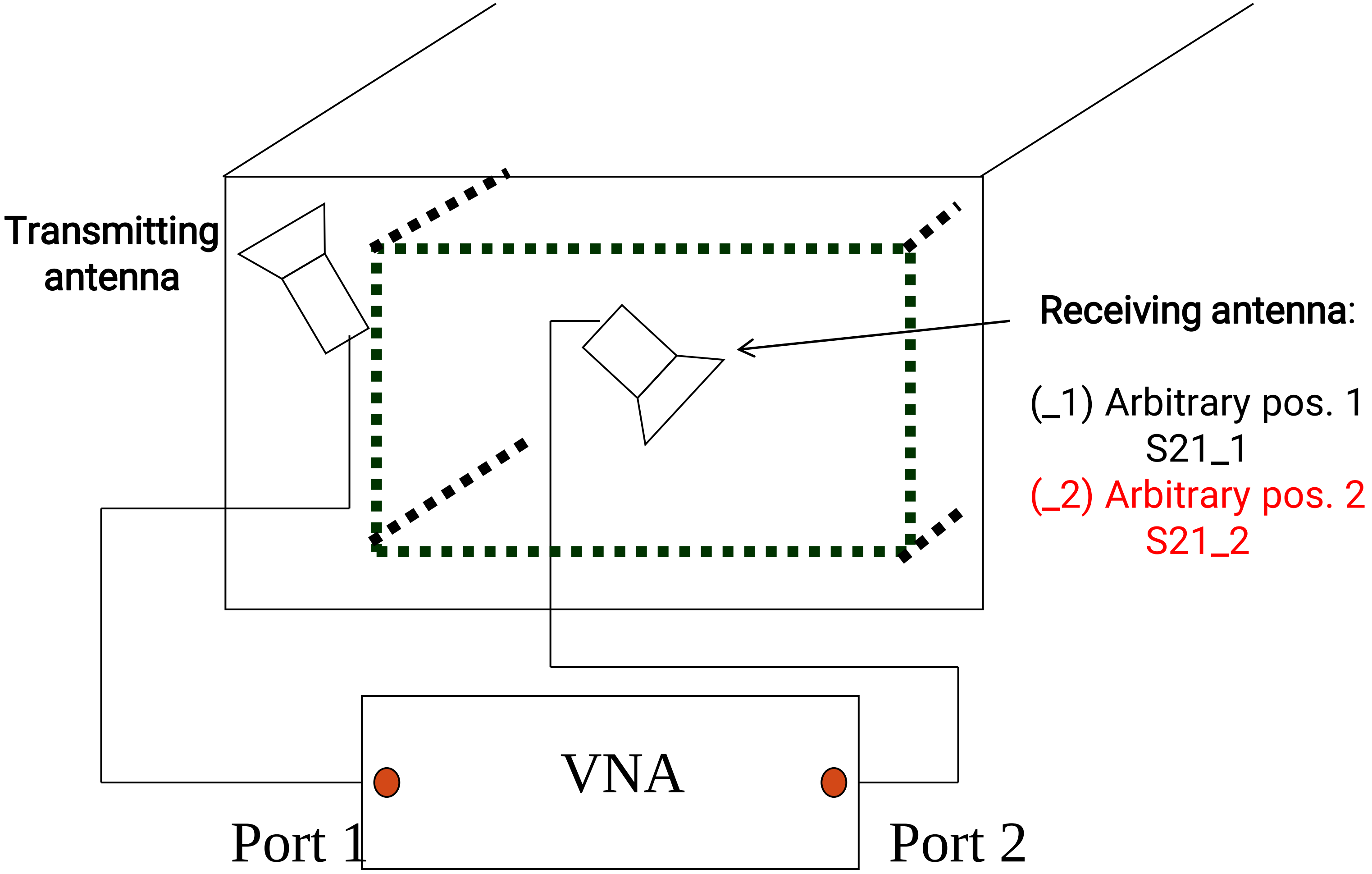

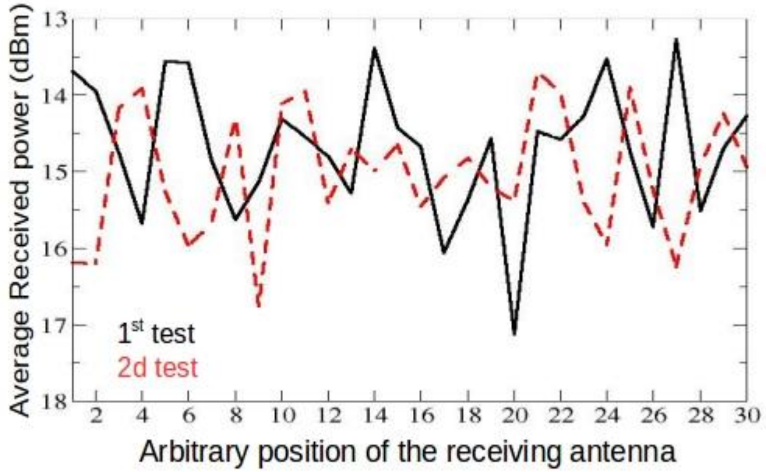

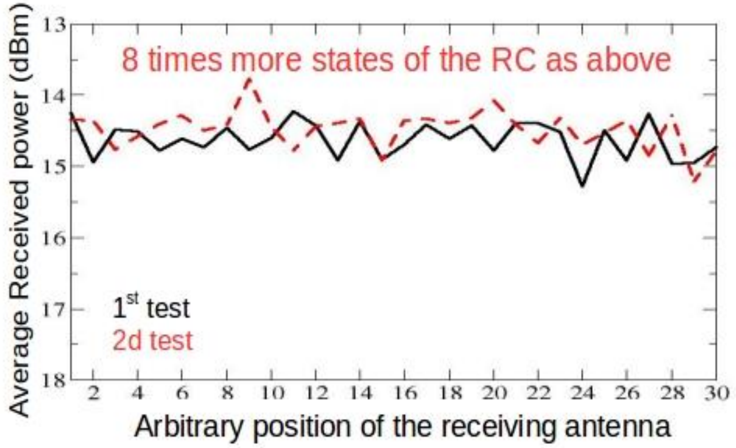

Antenna efficiency and antenna patterns in RC

Antenna efficiency from Q

$$Q_{1ant} = \left\langle \left| S_{xx} - \langle S_{xx} \rangle \right|^2 \right\rangle \frac{Z_0 \omega \epsilon V}{(\lambda^2/4\pi)(1 - |\langle S_{xx} \rangle|^2)^2 \eta_x^2}.$$

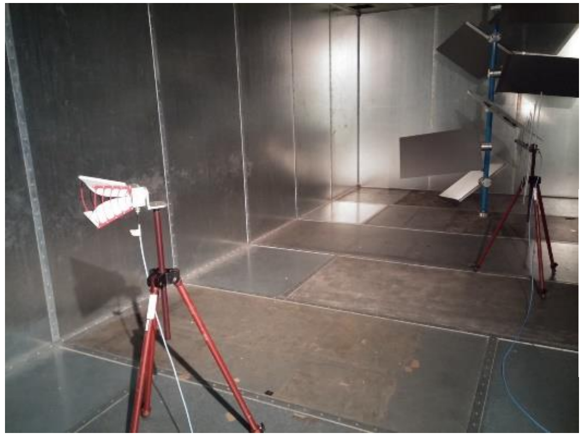

$$Q_x = \frac{Q_x^{\#}}{\eta_x^2}.$$

$$\eta_2 = \sqrt{\frac{Q_2^{\#}}{Q_1^{\#}}}\eta_1 = \sqrt{\frac{Q_2^{\#}}{Q_1}}$$

Q estimation at two identical antennas

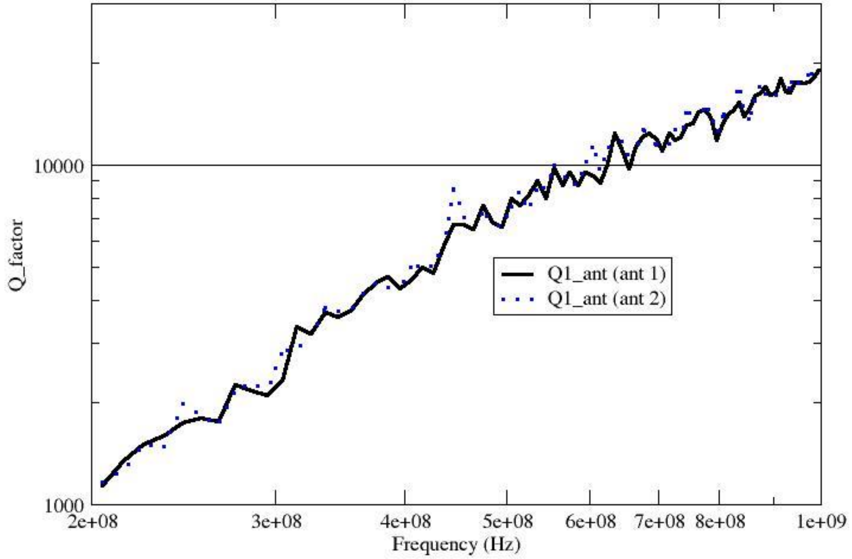

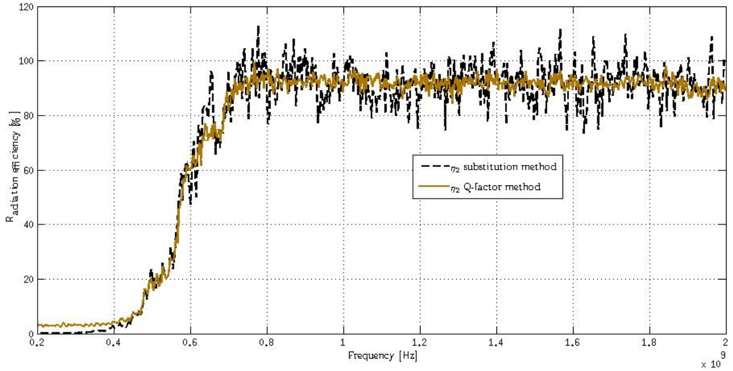

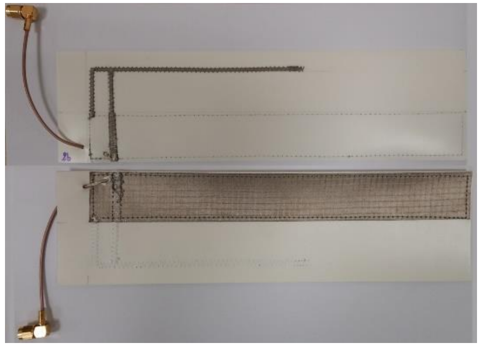

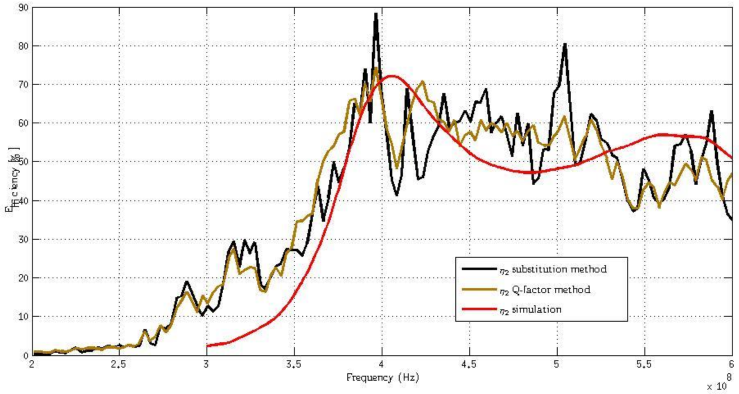

P. Besnier, J. Sol, A. Presse, C. Lemoine, and A. -C. Tarot, “Antenna efficiency measurement from quality factor estimation in reverberation chamber,” in *Proc. Eur. Microw. Conf.*, 2016, pp. 715–718,

Antenna efficiency and antenna patterns in RC

Antenna pattern

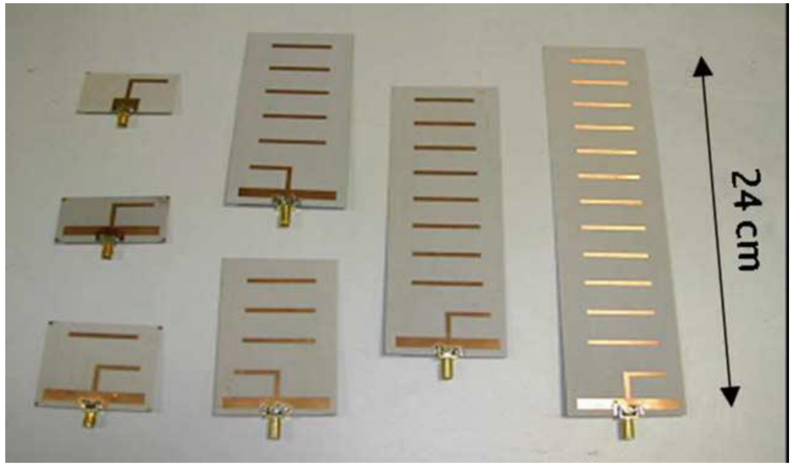

K factor
(Ricean channel)

$$K = \frac{v^2}{2\sigma^2}\cdot$$

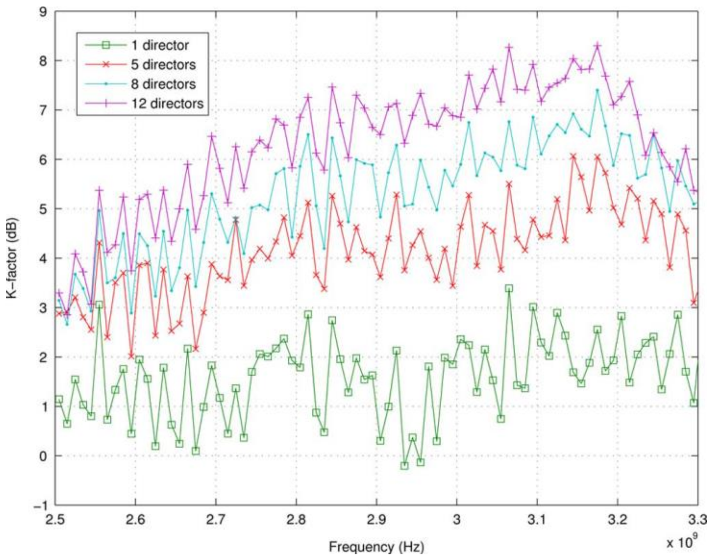

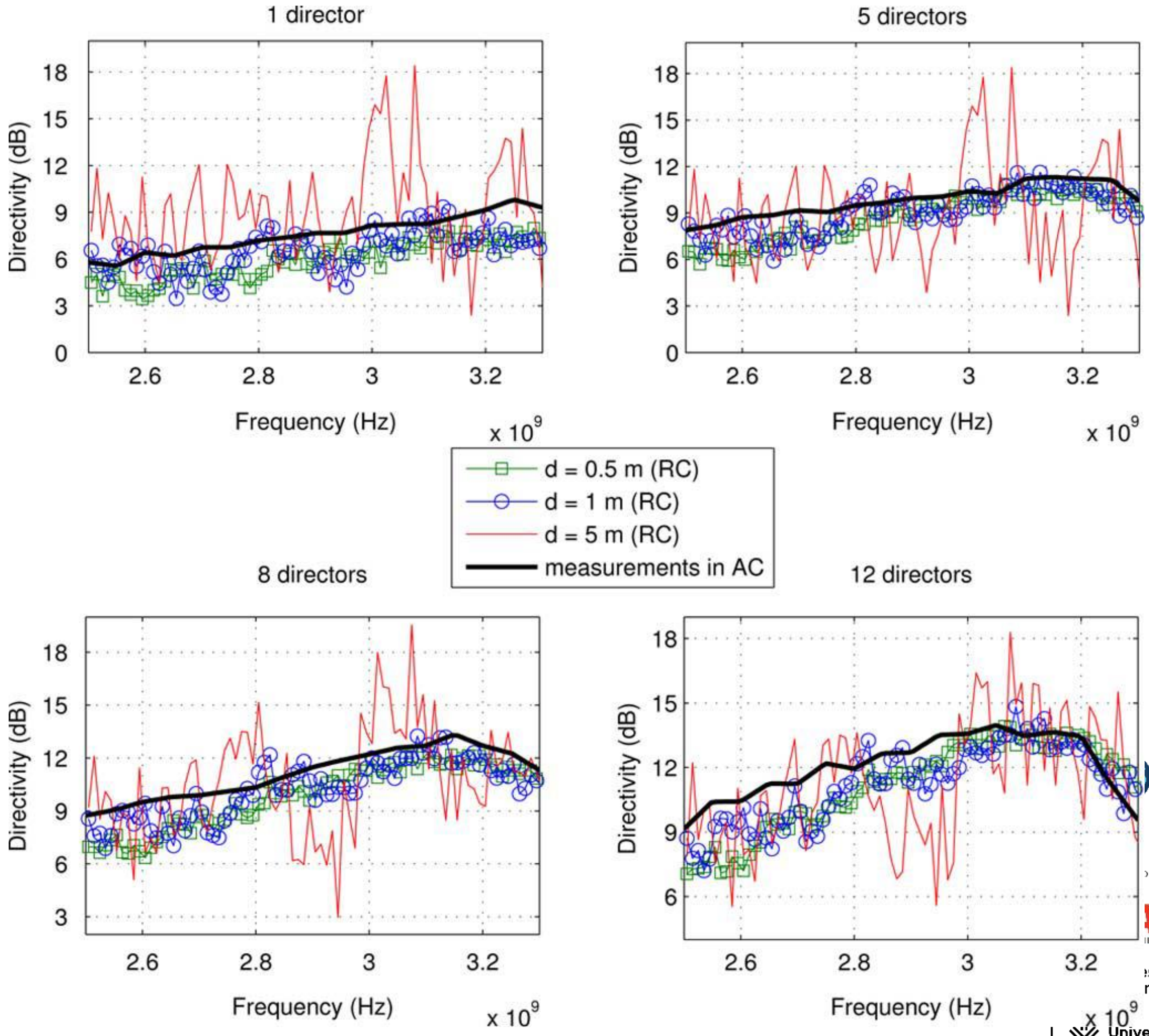

C. Lemoine, E. Amador, P. Besnier, J. -M. Floc'h and A. Laisné, "Antenna Directivity Measurement in Reverberation Chamber From Rician K-Factor Estimation," in *IEEE Transactions on Antennas and Propagation*, vol. 61, no. 10, pp. 5307-5310, Oct. 2013.

Average absorbing cross-section

$$P_{d-obj} = \sigma_{abs} \frac{E^2}{Z_0}.$$

$$Q_{obj} = \frac{2\pi V}{\lambda} \frac{1}{\sigma_{abs}}.$$

$$\sigma_{abs} = \frac{2\pi V}{\lambda} \left(\frac{1}{Q_g^L} - \frac{1}{Q_g^0}\right).$$

$$\sigma_{abs} = \langle T \rangle \frac{A_{tot}}{2}.$$

$$\langle T \rangle = 2 \int_0^{\pi/2} \left[1 - \frac{|\Gamma_{TM}(\theta)|^2 + |\Gamma_{TE}(\theta)|^2}{2}\right] \cos(\theta) \sin(\theta) d\theta.$$

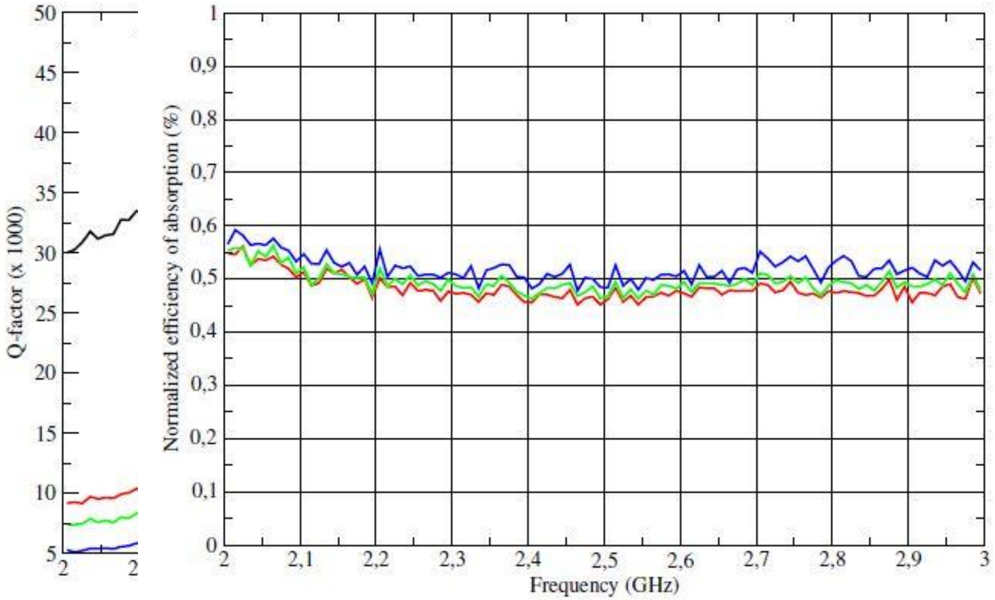

Andrieu, Guillaume (ed.): 'Electromagnetic Reverberation Chambers: Recent advances and innovative applications' (Electromagnetic Waves, 2020), IET

Dosimetry

$$\frac{\rho C}{k_t}\frac{\partial T}{\partial t} = \frac{\partial^2 T}{\partial x^2} + \frac{\partial^2 T}{\partial y^2} + \frac{\partial^2 T}{\partial z^2} - \frac{V_s}{k_t}(T - T_b) + \frac{q(x, y, z, t)}{k_t},$$

$$q(z) \simeq \frac{\langle S_0 \rangle \bar{T}_p}{\delta}\left[\exp(-2z/\delta) + \exp(-2(L_z - z)/\delta)\right].$$

(1D)

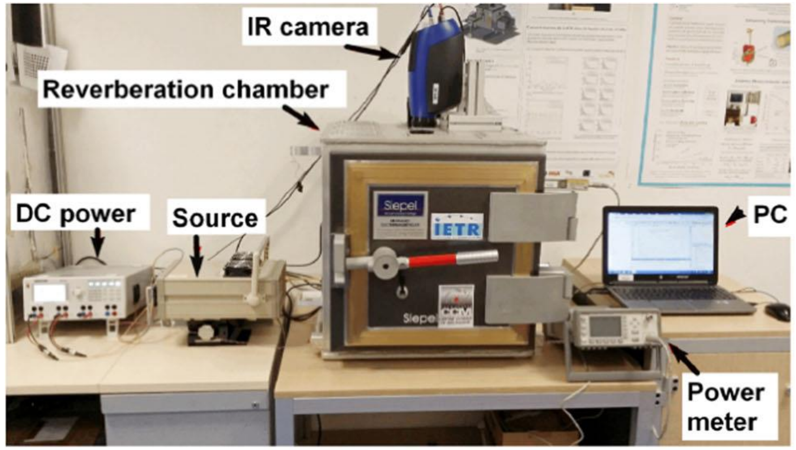

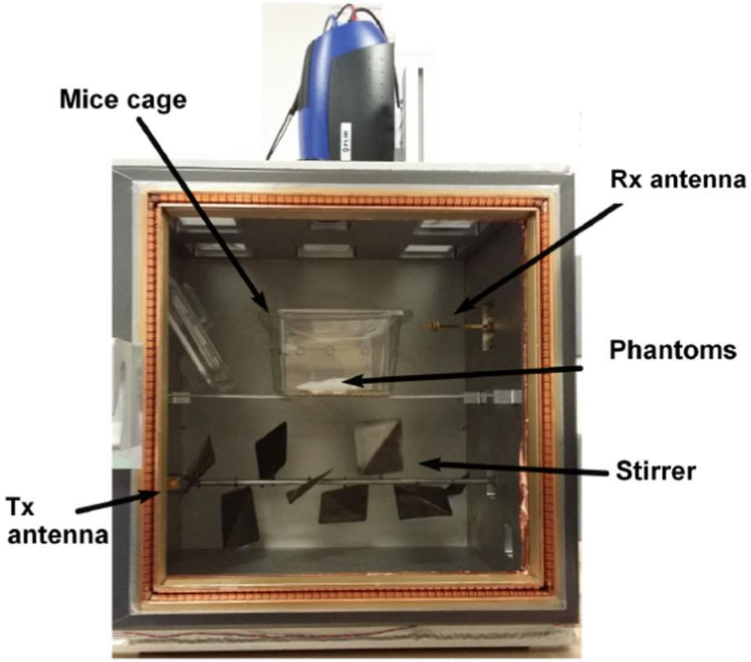

Khadir Fall, A. et al. (2020), Exposure Assessment in Millimeter-Wave Reverberation Chamber Using Murine Phantoms. Bioelectromagnetics, 41: 121-135

Comple

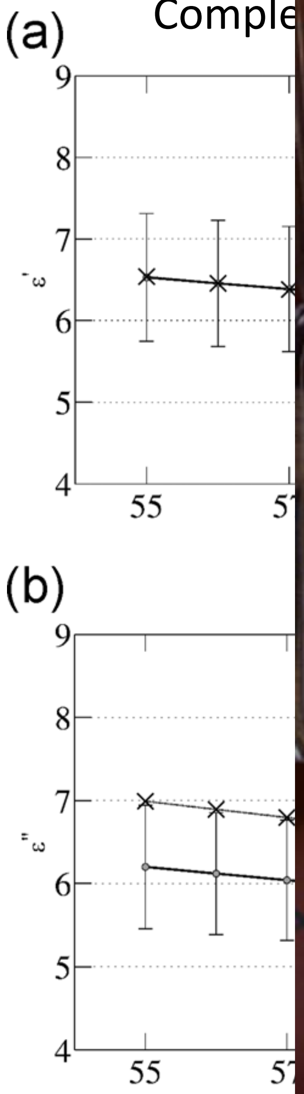

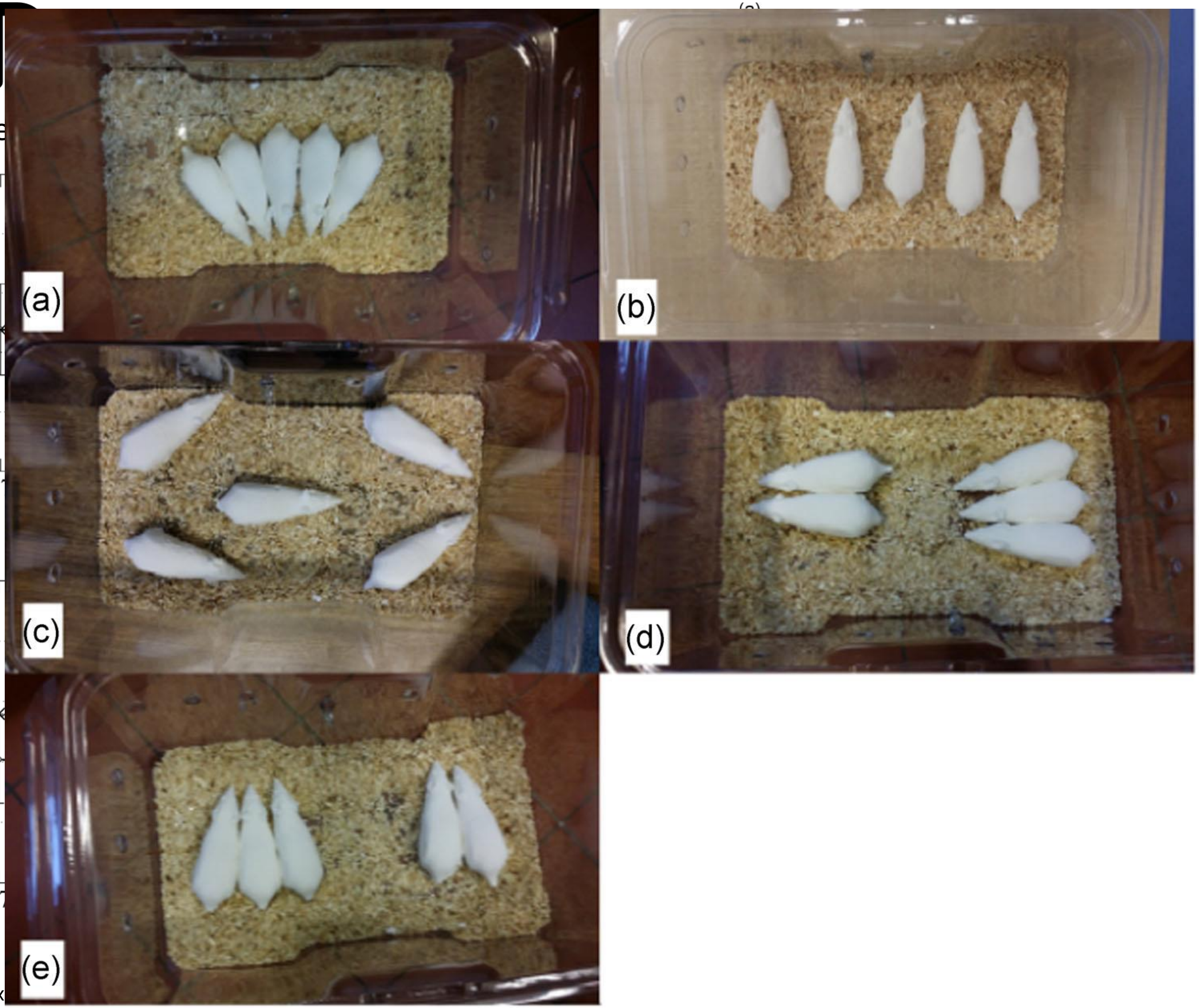

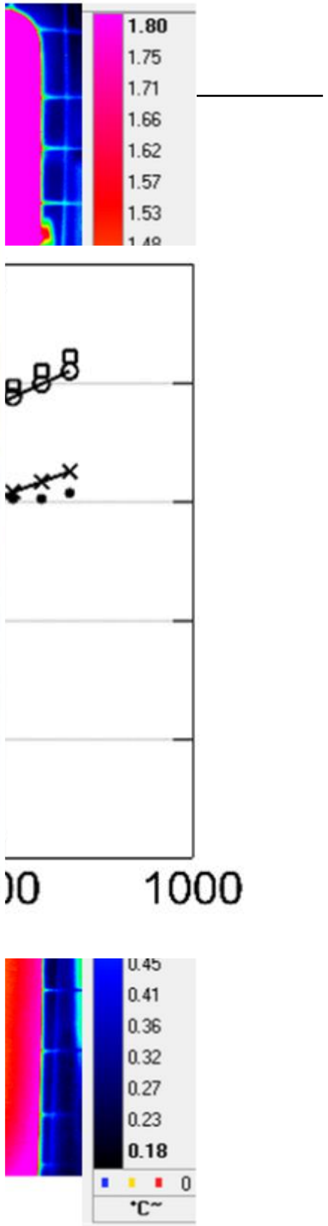

Khadir Fall, A. et al. (2020), Ex

Backscattering measurements

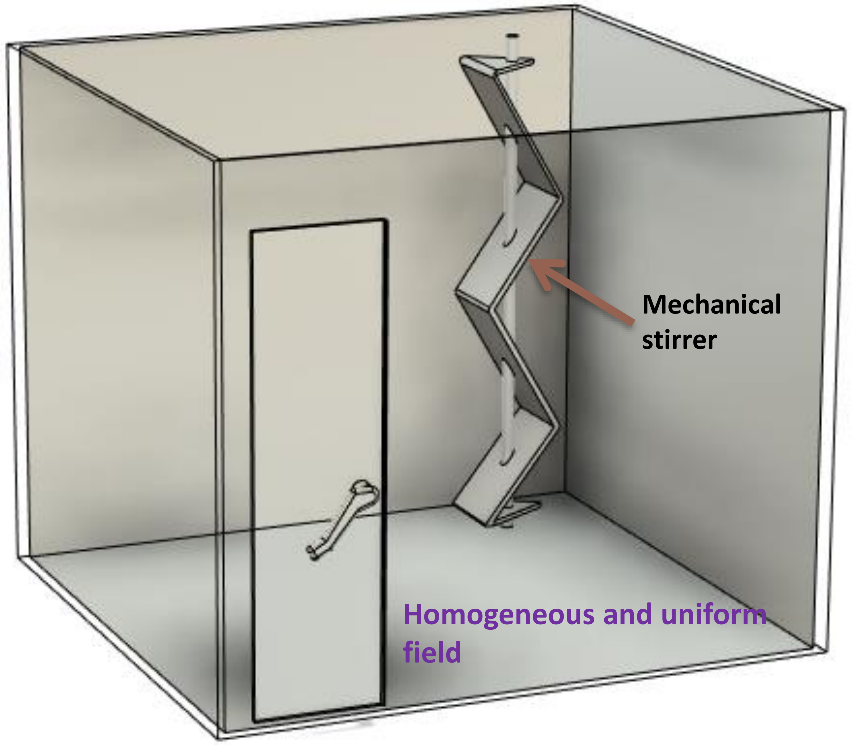

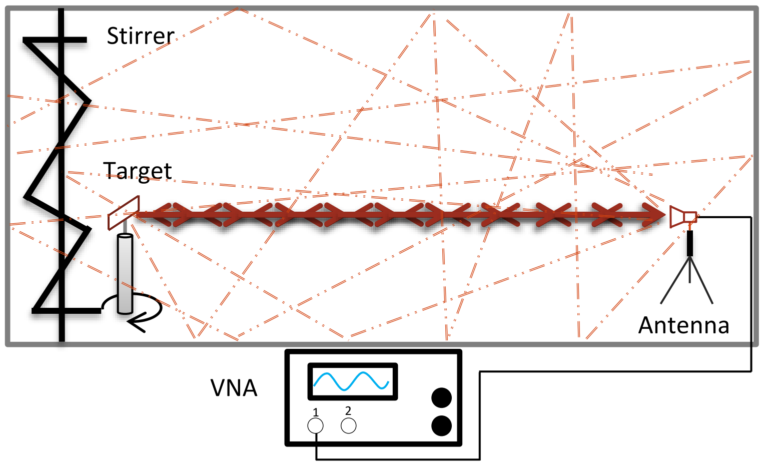

Multiple paths

LOS path extraction ?

Backscattering measurements

Mesure dans la chambre à vide (sans la cible):

$$S(f_0,\alpha_{br}) = S_{EL}(f_0) + (1-|S_{EL}(f_0)|^2)\eta_{ant}[H(f_0,\alpha_{br}) + h_s(f_0,\alpha_{br})]$$

Espace libre — Rétrodiffusion CRBM — Réflexions spéculaires

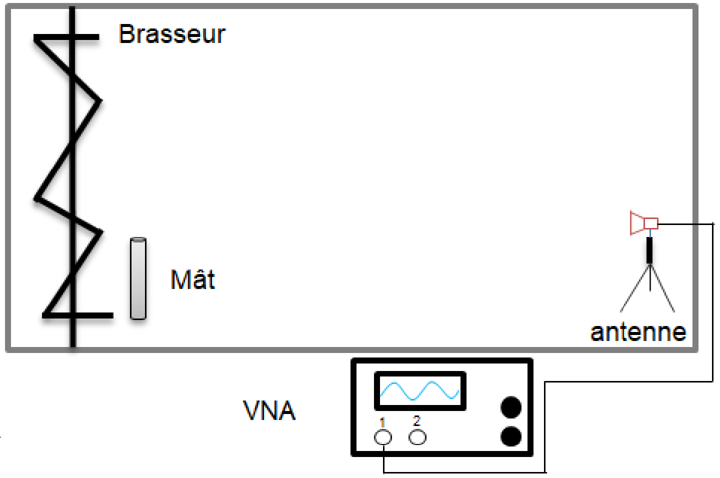

Mesure dans la chambre chargée (avec la cible):

$$S_c(f_0,\alpha_{br},\theta_c) = S_{EL}(f_0) + C(f_0)\sqrt{\sigma_c(f_0,\theta_c)} + (1-|S_{EL}(f_0)|^2)\eta_{ant}[H_c(f_0,\alpha_{br},\theta_c) + h_s(f_0,\alpha_{br})]$$

Espace libre — Onde balistique — Rétrodiffusion CRBM — Réflexions spéculaires

$$|C(f_0)| = \frac{G_{ant}(f_0)\lambda_0}{(4\pi)^{3/2}R^2}(1-|S_{EL}(f_0)|^2)$$

SER

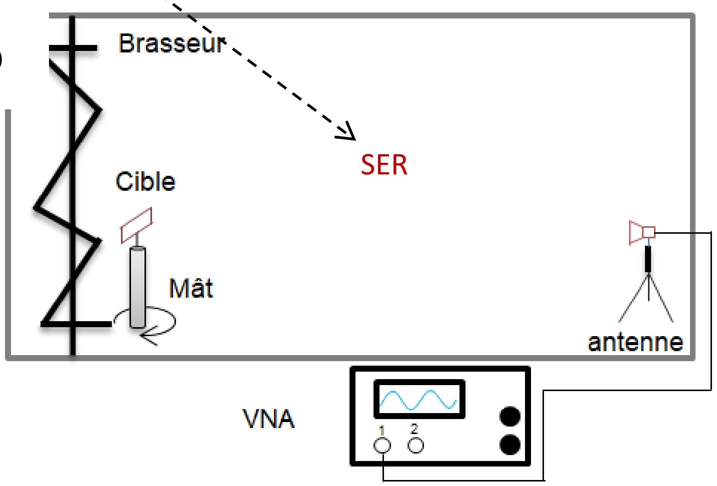

A. Reis *et al.*, "Radar Cross Section Pattern Measurements in a Mode-Stirred Reverberation Chamber: Theory and Experiments," in *IEEE Transactions on Antennas and Propagation*, vol. 69, no. 9, pp. 5942-5952, Sept. 2021.

Backscattering measurements

$$S_c(f_0,\alpha_{br},\theta_c) - S(f_0,\alpha_{br}) = \boxed{(1-|S_{EL}(f_0)|^2)\eta_{ant}\left[H_c(f_0,\alpha_{br},\theta_c) - H(f_0,\alpha_{br})\right]} + \boxed{\sqrt{\sigma_c(f_0,\theta_c)} \times |C(f_0)| \times exp\left[-j\left(2\pi f_0 \frac{2R}{c} - \phi_0\right)\right]}$$

Rétrodiffusion CRBM

SER

Amplitude onde balistique

- Extraction précise de l'amplitude
- Déduire la SER

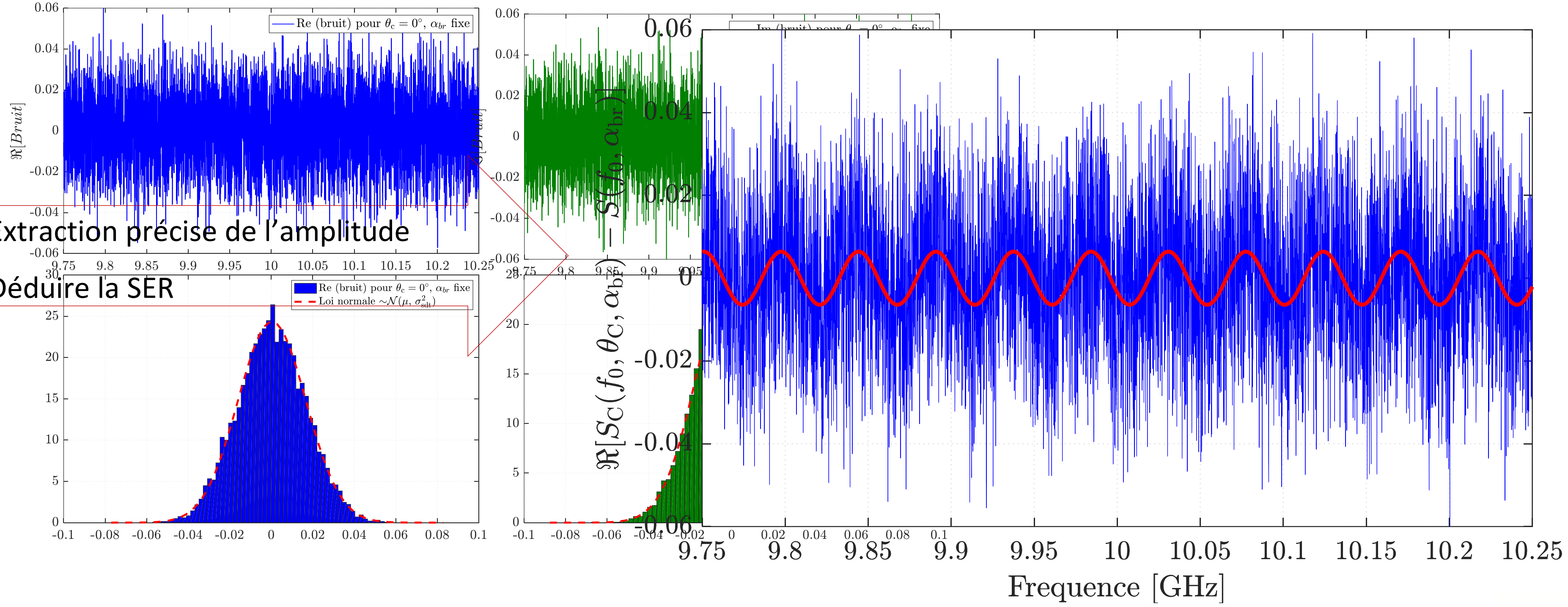

Backscattering measurements

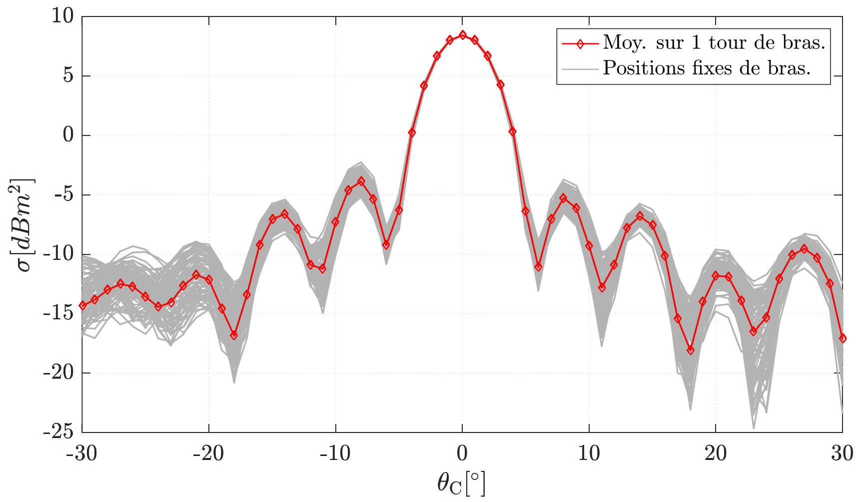

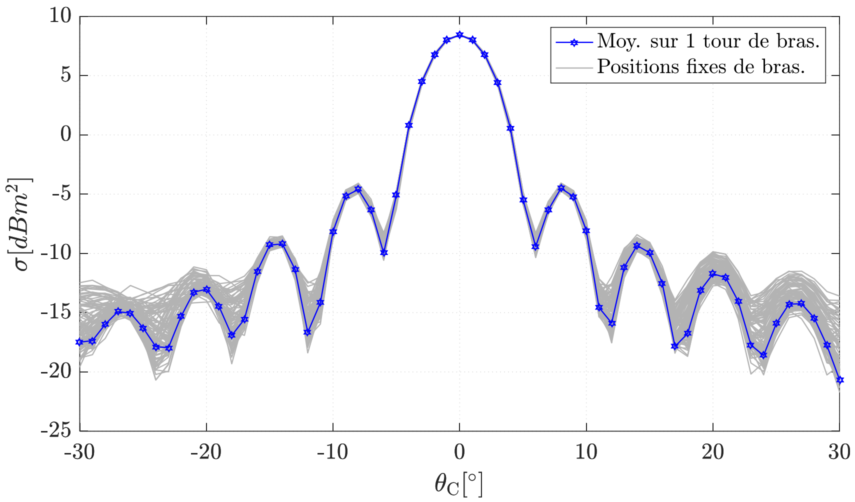

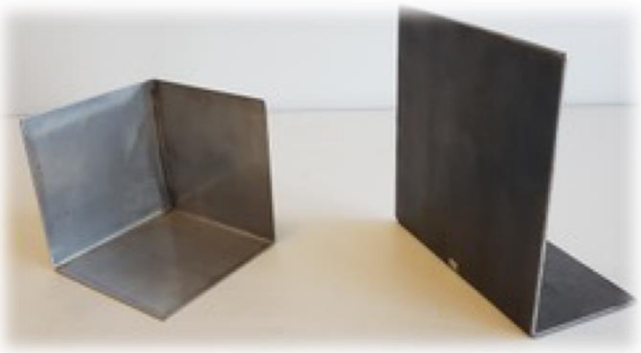

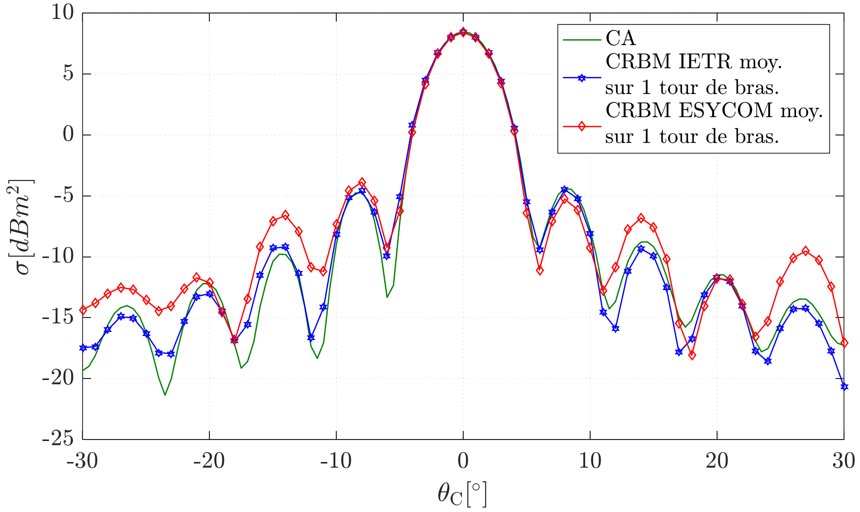

Backscattering measurements

Recent improvements

Quasi-monostatic configuration (no stirring)

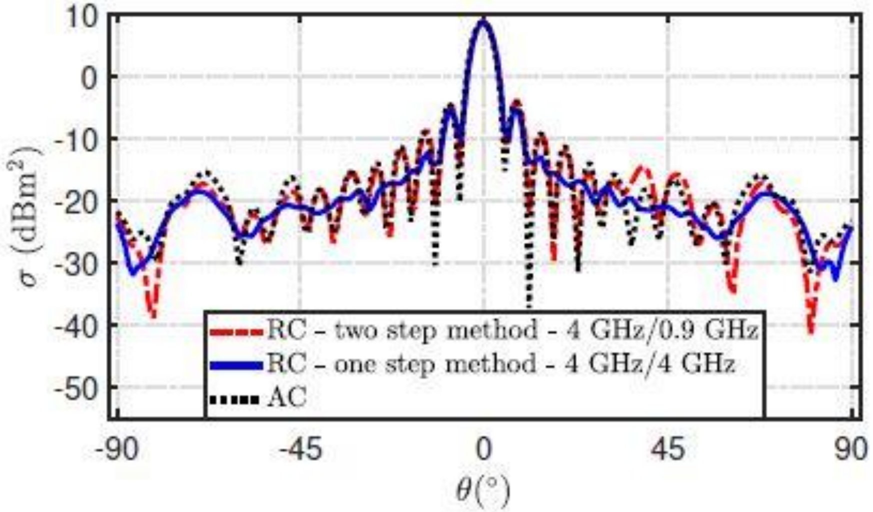

Distance
+
Amplitude

Charlo, C., Méric, S., Sarrazin, F., Richalot, E., Sol, J., & Besnier, P. (2023). Advanced Analysis of Radar Cross-Section Measurements in Reverberation Environment. https://arxiv.org/abs/2303.08751

Backscattering measurements

Antenna radar cross-section → Antenna pattern ?

$$\sqrt{\sigma_{\mathrm{ant}}} = \sqrt{\sigma_{\mathrm{s}}} + \sqrt{\sigma_{\mathrm{r}}}$$

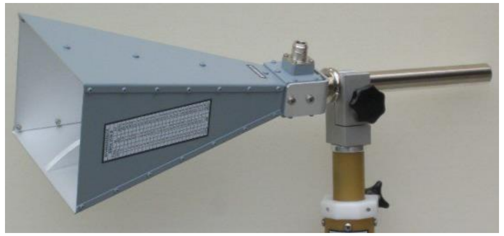

Radiating mode

$$\sqrt{\sigma_{\mathrm{r}}} = \sqrt{\sigma_r^{\max}} \cdot |\Gamma_{\mathrm{L}}|$$

Measurements with two loads L1 and L2:

$$S_{\mathrm{L1}} = S_{\mathrm{FS}} + (1 - |S_{\mathrm{FS}}|^2)\eta_a H_{\mathrm{L1}} + \mathrm{C}\left(\sqrt{\sigma_{\mathrm{s}}} + \sqrt{\sigma_r^{max}} \cdot |\Gamma_{\mathrm{L1}}|\right)$$

$$S_{\mathrm{L2}} = S_{\mathrm{FS}} + (1 - |S_{\mathrm{FS}}|^2)\eta_a H_{\mathrm{L2}} + \mathrm{C}\left(\sqrt{\sigma_{\mathrm{s}}} + \sqrt{\sigma_r^{max}} \cdot |\Gamma_{\mathrm{L2}}|\right)$$

$$S_{\mathrm{L1}} - S_{\mathrm{L2}} = (1 - |S_{\mathrm{FS}}|^2)\eta_a (H_{\mathrm{L1}} - H_{\mathrm{L2}}) + \mathrm{C}\sqrt{\sigma_r^{max}} \cdot (|\Gamma_{\mathrm{L1}}| - |\Gamma_{\mathrm{L2}}|)$$

Backscattering measurements

$$S_{L1} - S_{L2} = (1 - |S_{FS}|^2)\eta_a(H_{L1} - H_{L2}) + |C|\sqrt{\sigma_r^{max}}(|\Gamma_{L1}| - |\Gamma_{L2}|)\, exp\, \frac{-j2\pi f 2R}{c}$$

$$\Delta_S = \sqrt{\sigma_r^{max}}\, exp\left(-j2\pi f\, \frac{2R}{c}\right) + noise$$

72 stirring positions
+
sinusoidal regression

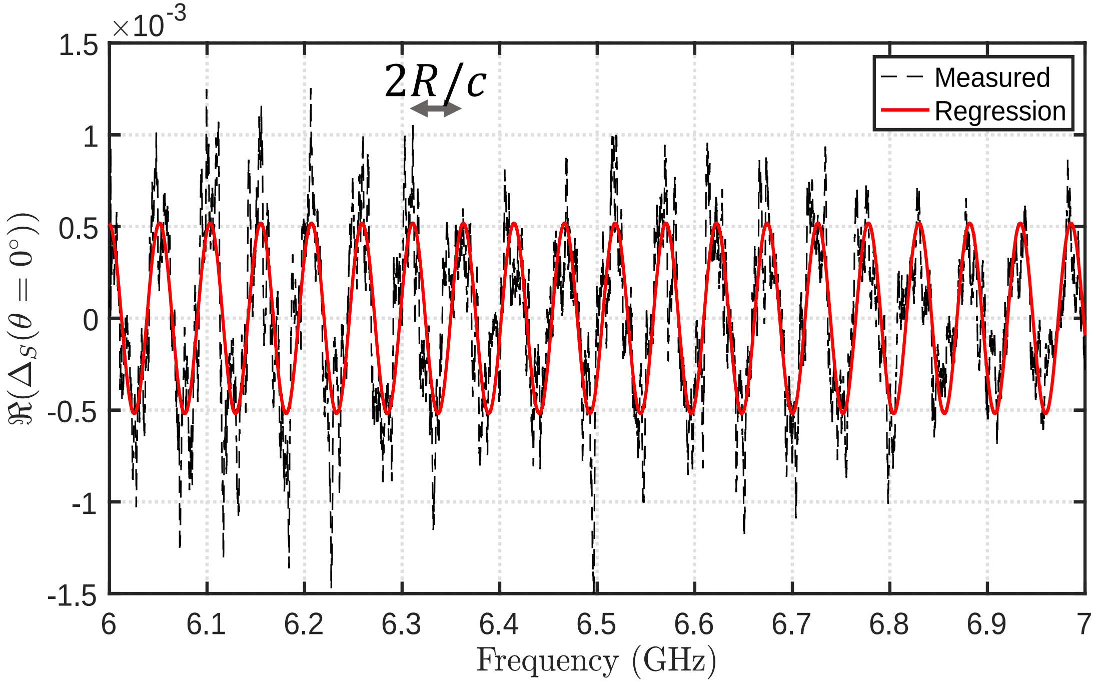

Backscattering measurements

Validation ESYCOM RC 19 m³

Fréquency: [6-7] GHz

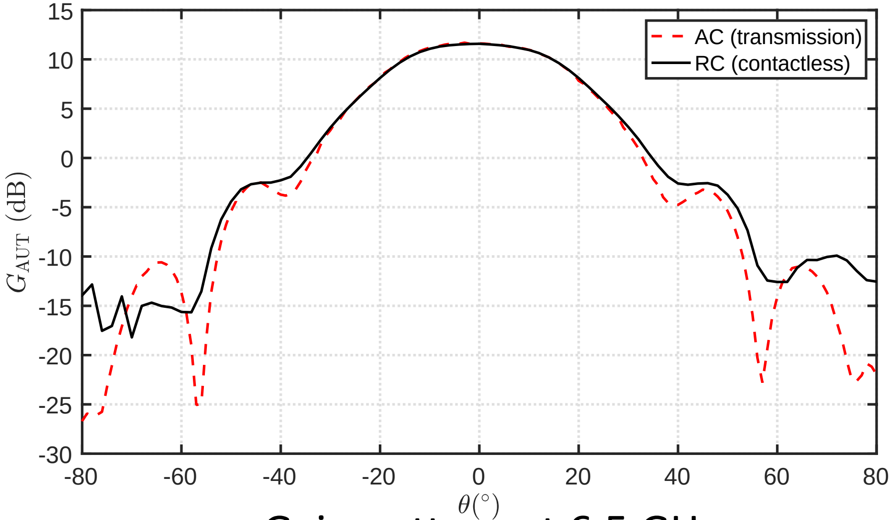

Gain pattern at 6.5 GHz

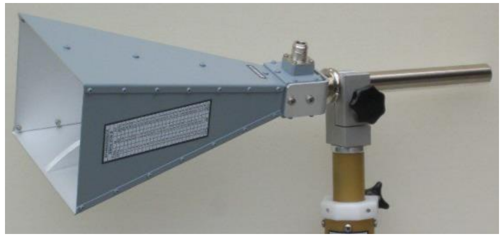

Fréquency: [3-4] GHz

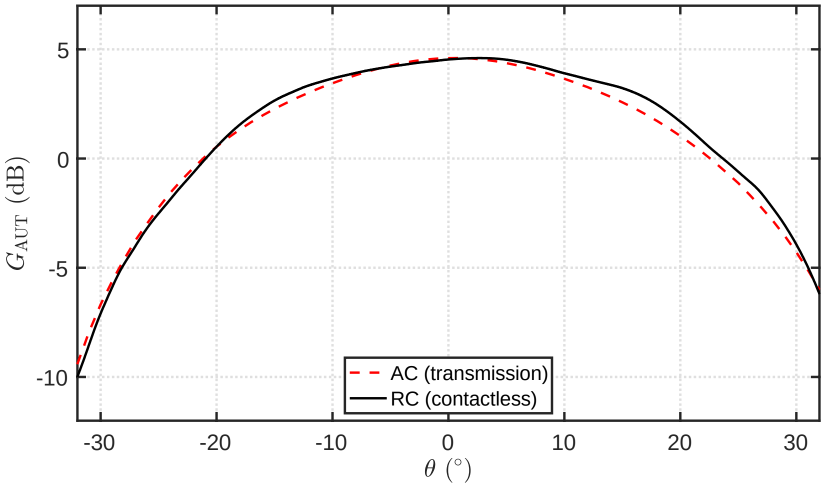

[5] A. Reis, F. Sarrazin, P. Besnier, P. Pouliguen and E. Richalot, "Contactless Antenna Gain Pattern Estimation From Backscattering Coefficient Measurement Performed Within a Reverberation Chamber," in *IEEE Transactions on Antennas and Propagation*, vol. 70, no. 3, pp. 2318-2321, March 2022, doi: 10.1109/TAP.2021.3111184.

Focalization

Focalization upon detection of the modification of the backscattered field
(opérateur de Wigner-Smith généralisé)

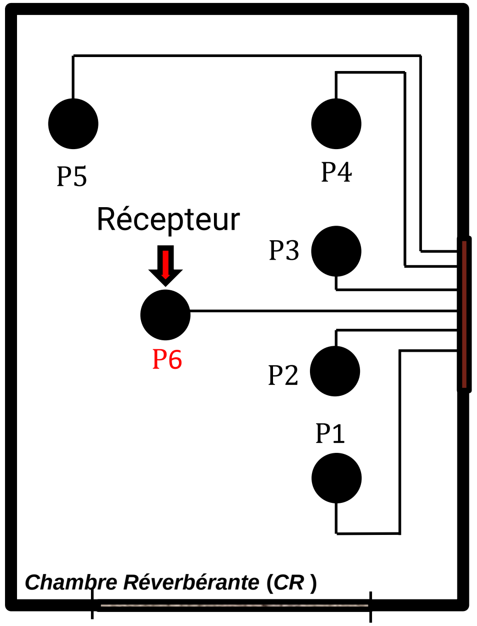

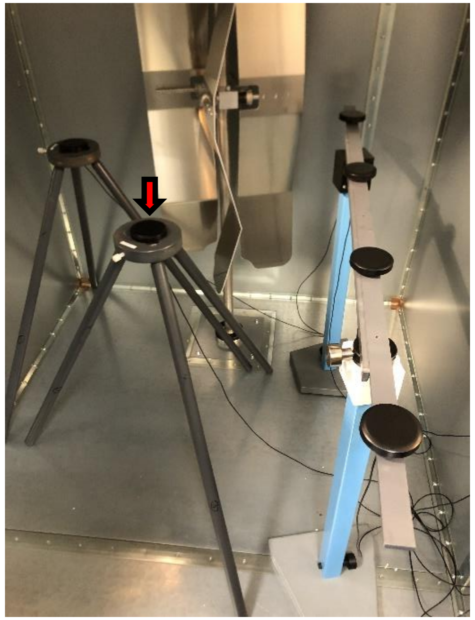

Connection

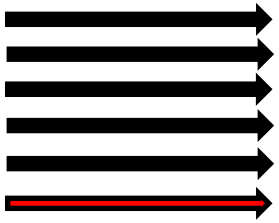

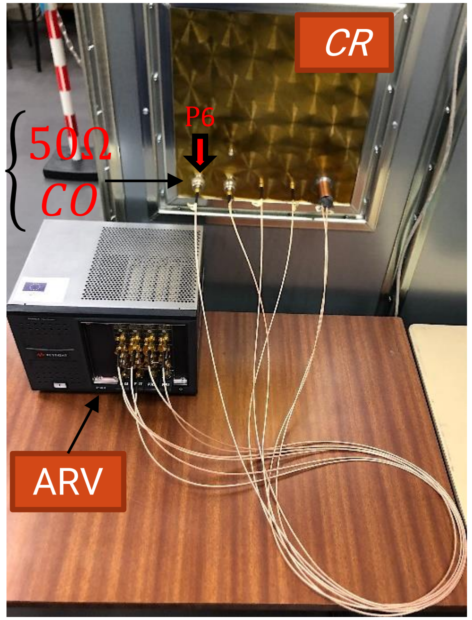

- Impedance modification: 50 Ω (S_1) and CO (S_2) ➔ $Q_\alpha = -iS_1^{-1}(S_1 - S_2)$
- Diagonalization of Q_α➔ q_i with the highest $|\lambda_i|$ -> Most sensitive to the change
- Injection de q_i à l'émission ➔ focalisation

Focalization

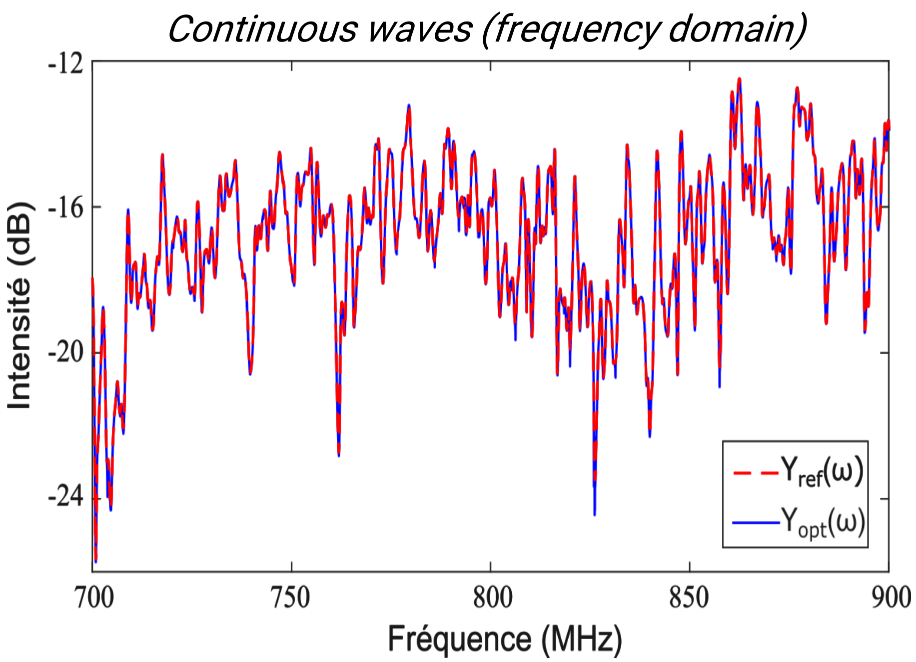

- $Y_{ref}(\omega) = \left|\psi_{ref}(\omega)t(\omega)\right|^2 = \|T\|^2$, PHASE CONJUGATION
- $Y_{opt}(\omega) = \left|\psi_{opt}(\omega)T(\omega)\right|^2$, avec $\psi_{opt} = q_1^T$; WSG FOCALIZATION

Focalization (time domain, in situ)

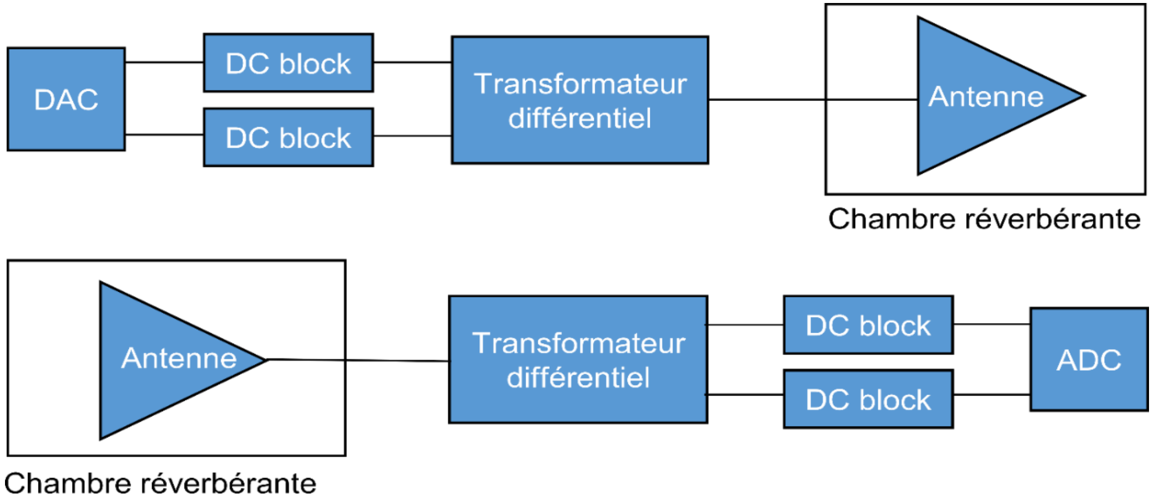

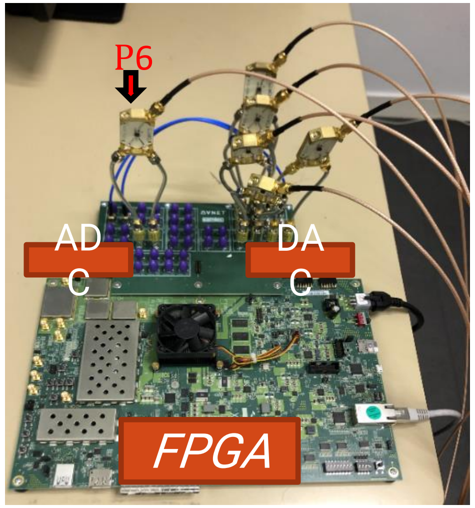

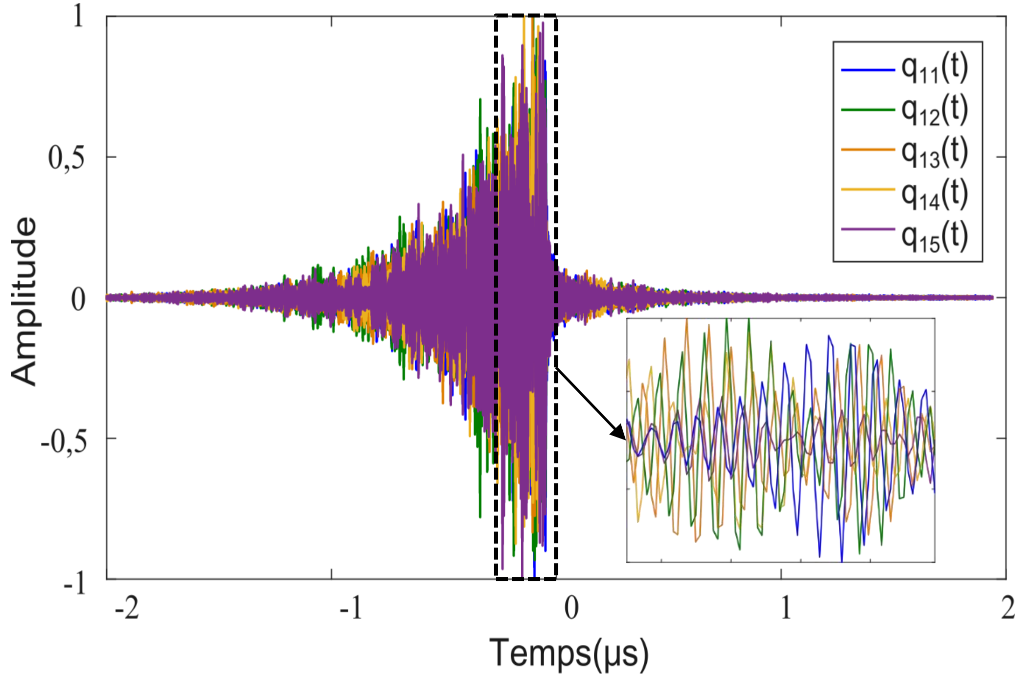

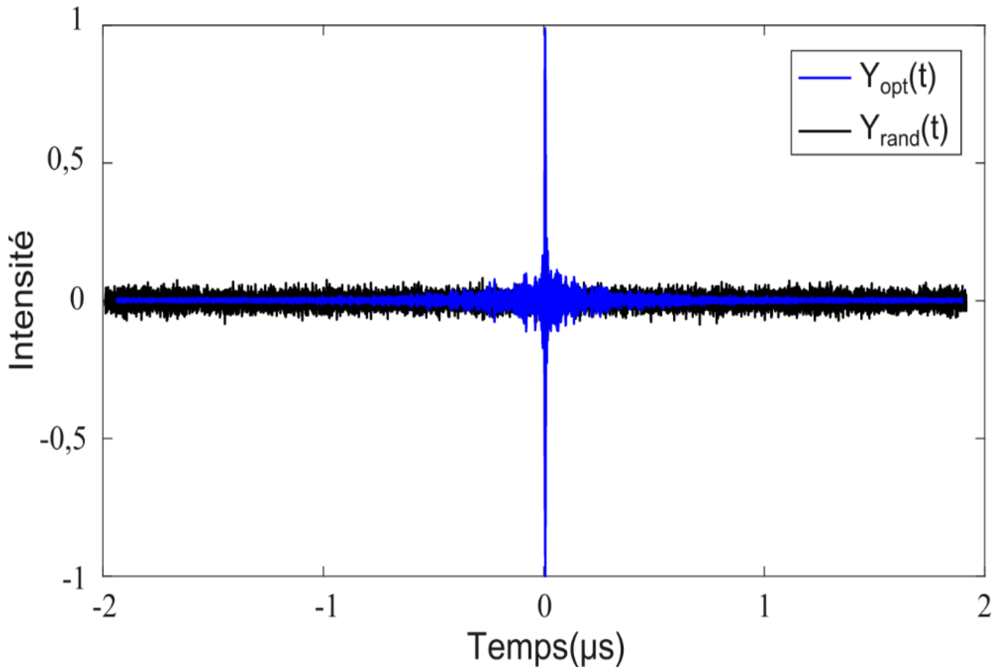

K. B. Yeo, C. Leconte, P. del Hougne, P. Besnier and M. Davy, "Time Reversal Communications With Channel State Information Estimated From Impedance Modulation at the Receiver," in *IEEE Access*, vol. 10, pp. 91119-91126, 2022

Conclusion

Reverberation chambers have remarkable properties for radiofrequency test purposes

Its usage extends from EMC applications (historical applications) to various RF applications

- Antennas (efficiency, pattern) including passive antenna measuremnts
- Dosimetry
- Radar cross section
- Time reversal / focalization experiments

Foreseen applications (research works)

- Improvements of passive antennas characterizations and RCS measurement accuracy
- RIS performance assessment
- Recent ideas for non-invasive shielding effectiveness estimation

PhD offer

Contactless Characterization of Miniature and Buried Antennas Within Reverberation Chambers

Supervision François Sarrazin: Junior Professor Chair at Université de Rennes
Philippe Besnier: Research Director at CNRS

Keywords: Antenna characterization, Miniature antenna, Reverberation chamber

Context: Smart cities rely on the use on wireless sensor networks to ensure monitoring activities for a large panel of applications: structural health, soil composition, air, and water quality… Sensors are therefore either in contact or embedded within a lossy medium such as concrete, soil or water. Such complex environment in the sensor's vicinity implies a degradation of the radio performances, and particularly a decrease in the antenna radiation efficiency. The estimation of such efficiency, critical parameter to limit power consumption, is barely possible with conventional measurement methods in the case of buried and miniature antennas. Indeed, conventional measurement approaches necessitate to connect the antenna under test to an analyzer whereas the presence of the cables in the antenna reactive near-field zone disturbs the radiation and impedance properties [1]. In that context, innovative efficiency measurement methods are required to overcome current limitations of conventional methods.

PhD Offer

Keyboard Compromission Through Electromagnetic Attacks using Wavefront Shaping

Supervision François Sarrazin: Junior Professor Chair at Université de Rennes
Philippe Besnier: Research Director at CNRS

Keywords: Electromagnetic compatibility/cybersecurity, Wave control, Fault-injection

PhD Context: Electromagnetic cybersecurity relates to the use of electromagnetic waves to compromise data. Keyboards are critical targets because they are widely used as a computer peripheral and keystroke retrieval may lead to sensitive information recovery. Various attacks have been proposed to remotely retrieve keystrokes by listening to electromagnetic emanations either in a passive [Vua09] or active [Kaj23] manner using backscattering measurement. However, the feasibility of denial-of-service attacks on computer keyboard remains an open challenge.

CNRS Images. © Jean-Claude MOSCHETTI / IETR / CNRS Photothèque

IETR

Many thanks to collaborators at IETR, ESYCOM, Institut Langevin, INPHYNI …

cnrs
CentraleSupélec
INSA RENNES
Nantes Université
Université de Rennes